J. Fluid Mech. (1984), *vol.* 142, *pp.* 171–186
Printed in Great Britain

On the stability of an axisymmetric plume in a uniform stream

By D. S. RILEY AND M. TVEITEREID†
School of Mathematics, University of Bristol, England

(Received 18 April 1983 and in revised form 6 January 1984)

The linear stability equations for a round laminar thermal plume in a coflowing vertical stream have been solved numerically. Both symmetric and asymmetric disturbances have been considered for strengths of the forced flow varying between very weak and very strong. The parallel flow analysis confirms that the forced flow has a stabilizing effect. The upper branch of the neutral curve for sinuous disturbances is qualitatively like that of a round momentum jet. However, neither a critical Reynolds number nor a lower branch of the neutral curve was found. Non-parallel effects are discussed.

1. Introduction

The stability of certain axisymmetric flows, round jets and Poiseuille flow in particular, has been extensively studied, using both linear and nonlinear stability theory. The first theoretical study of the stability of axisymmetric free flows was carried out by Batchelor & Gill (1962), who considered the linear stability of jets in an inviscid fluid. They found that a thin momentum jet is unstable only to sinuous disturbances i.e. those with unit azimuthal wavenumber. Burridge (1968, 1970) made a comprehensive analytical and numerical attack on the corresponding viscous problem. He again used linear stability theory and confirmed the result of Batchelor & Gill that there was instability only to the sinuous disturbance. Burridge's calculations yielded a critical Reynolds number of 37.5 at a wavenumber of 0.43. There have been numerous other investigations, many of which were reviewed by Mollendorf & Gebhart (1973) in their numerical and experimental study of the vertical round jet with and without buoyancy.

In comparison to the jet problem, the related problem of the stability of the free convection flow above a point heat source has been neglected. The plume stability was first considered briefly by Mollendorf & Gebhart, who noted that their results concerning jets were applicable to an axisymmetric thermal plume with Prandtl number 2, because the velocity and temperature base profiles were then identical with those for a non-buoyant jet. There does not appear to have been any further theoretical attack on this problem until Wakitani (1980) investigated, again numerically, for Prandtl numbers of 2 and 0.7. As above, Wakitani found instability only for the sinuous mode, but seemingly because of difficulties with convergence of his numerical scheme, neither a critical Grashof number nor a lower branch of the neutral curve was found. Fujii, Morioka & Suzaki (1972) and Schlien & Boxman (1979) described their experiments on the stability of an axisymmetric plume in water.

Plume stability and transition are important questions in themselves. It is known

† Present address: Adger College of Engineering, AID-4890 Grimstad, Norway.

that the characteristics of flow vary widely between laminar and turbulent regimes and so it is important to understand each. Often in applications and in experiments it is desirable to preserve the laminar nature of the plume. In fact, the problem investigated in this paper originally arose when preliminary details of an experiment,† involving velocity measurements in a thermal plume, came to our attention. It seems that to stabilize an axisymmetric plume it requires only a small imposed external stream aligned with the axis of the plume. It is natural to enquire why and how this happens. It is plausible that a plume should be stabilized in this way, because it may be expected that, by so doing, the degree of inflexion is lessened. This, however, cannot be the complete story, since it is known from previous stability studies in free convection that there are two distinct mechanisms for instability. The first is hydrodynamical and is the one usually associated with inflexion points and with the Orr–Somerfield equation; the other is buoyancy. Thus in this paper we set out to examine the effects of an aligned uniform (coflowing) stream on the stability characteristics of a thermal plume.

The basic flow for this problem was the subject of an investigation by Riley & Drake (1983). Here we first present details of the basic flow and then the linear stability equations. We discuss the eigenvalue problem, its solution and ramifications. Finally, we consider the balance of energy within the perturbation. The details of the numerical solutions are relegated to the Appendix.

2. The basic flow

The axisymmetric mixed convection flow results from a vertical uniform stream, of speed W_∞ and at temperature T_∞, passing over a point heat source. To describe the flow, cylindrical polar coordinates (r, ϕ, z) are employed, with the origin located at the heat source and with the z-axis pointing vertically upwards. r is the distance from the z-axis and ϕ is the angular coordinate. Furthermore we introduce T as the temperature and $\boldsymbol{V} = (U, 0, W)$ as the velocity vector, where U and W are the radial and vertical components, respectively.

On taking the Boussinesq form of the governing equations, they become

$$\frac{\partial}{\partial r}(rU)+\frac{\partial}{\partial z}(rW) = 0, \tag{2.1}$$

$$U\frac{\partial U}{\partial r}+W\frac{\partial U}{\partial z} = -\frac{1}{\rho}\frac{\partial p}{\partial r}+\nu\nabla^2 U, \tag{2.2}$$

$$U\frac{\partial W}{\partial r}+W\frac{\partial W}{\partial z} = -\frac{1}{\rho}\frac{\partial p}{\partial z}+\nu\nabla^2 W+g\beta(T-T_\infty), \tag{2.3}$$

$$U\frac{\partial T}{\partial r}+W\frac{\partial T}{\partial z} = \kappa\nabla^2 T. \tag{2.4}$$

Here p is the pressure, ν the kinematic viscosity, κ the thermal diffusivity, ρ the density, g the acceleration due to gravity and β the coefficient of cubical expansion. ∇^2 denotes the Laplacian in the cylindrical coordinates (r, z).

Symmetry about $r = 0$ gives, for $z \neq 0$,

$$U = 0, \quad \frac{\partial W}{\partial r} = 0, \quad \frac{\partial T}{\partial r} = 0, \tag{2.5}$$

† Unfortunately, the experiment was primarily concerned with the measurements of gas velocities and temperatures within the plume, and stability *per se* was not considered.

whilst far away from the heat source the velocity and temperature must attain the same values as in the imposed flow, i.e.

$$W \to W_\infty, \quad T \to T_\infty \quad \text{as} \quad r \to \infty. \tag{2.6}$$

Finally, the heat flux across a sphere centred at the heat source must be equal to the strength of the source:

$$\iint_{\text{sphere}} \boldsymbol{q}\cdot\boldsymbol{n}\,\mathrm{d}S = Q, \tag{2.7}$$

where $\boldsymbol{n}$ denotes the outward normal to the sphere, $\boldsymbol{q}$ the total heat-flux vector and Q is the strength of the heat source.

On using tildes to denote quantities non-dimensionalized by use of a characteristic speed U^*, length L^* and temperature difference T^* defined by

$$U^* = \left(\frac{\beta g Q}{2\pi\rho c_p \nu}\right)^{\frac{1}{2}}, \quad L^* = \left(\frac{288\pi\rho c_p \nu^3}{g\beta Q}\right)^{\frac{1}{2}}, \quad T^* = \frac{Q}{24\pi\rho c_p \nu^2 L^*}, \tag{2.8}$$

where c_p denotes specific heat, attention is restricted to the shear-layer region where $\eta = \tilde{r}/\tilde{z}^{\frac{1}{2}}$ is $O(1)$ as $\tilde{z}\to\infty$. The solutions to (2.1)–(2.7) have the following asymptotic expansions valid in this region:

$$\left.\begin{aligned} \tilde{S} &= \tilde{z}F(\eta) + O(\tilde{z}^{\frac{1}{2}}), \\ \tilde{\theta} &= \tilde{z}^{-1}H(\eta) + O(\tilde{z}^{-\frac{3}{2}}) \qquad \text{as} \quad \tilde{z}\to\infty, \end{aligned}\right\} \tag{2.9}$$

where $\tilde{S}$ is a (dimensionless) Stokes stream function such that

$$\tilde{r}\tilde{U} = -\frac{\partial\tilde{S}}{\partial\tilde{z}}, \quad \tilde{r}\tilde{W} = \frac{\partial\tilde{S}}{\partial\tilde{r}}$$

and

$$T - T_\infty = T^*\tilde{\theta}.$$

The governing system for F and H is

$$\left.\begin{aligned} \left(\eta\left(\frac{F'}{\eta}\right)'\right)' + 12F\left(\frac{F'}{\eta}\right)' + \eta H = 0, \\ (\eta H')' + 12\sigma(FH)' = 0, \end{aligned}\right\} \tag{2.10}$$

with

$$\left.\begin{aligned} &\lim_{\eta\to 0}\left(\frac{F'}{\eta}\right)' = F(0) = H'(0) = 0, \\ &\frac{F'}{\eta}\to\epsilon, \quad H\to 0 \quad \text{as} \quad \eta\to\infty, \\ &\int_0^\infty F'H\,\mathrm{d}\eta = 1. \end{aligned}\right\} \tag{2.11}$$

Here $\sigma = \nu/\kappa$ is the Prandtl number and $\epsilon = W_\infty/U^*$ is a measure of the strengths of the imposed flow relative to the natural convection.

Solutions to the above system were found by Riley & Drake, who used a similarity variable proportional to r^2/z rather than $r/z^{\frac{1}{2}}$; in this investigation, however, it proves more convenient to use the latter.

In the case of no imposed flow ($\epsilon = 0$) and $\sigma = 1$, a closed-form solution exists (Yih 1977, chap. 8):

$$F = \frac{\eta^2}{2(1+\eta^2)}, \quad H = \left(\frac{2}{1+\eta^2}\right)^3, \tag{2.12}$$

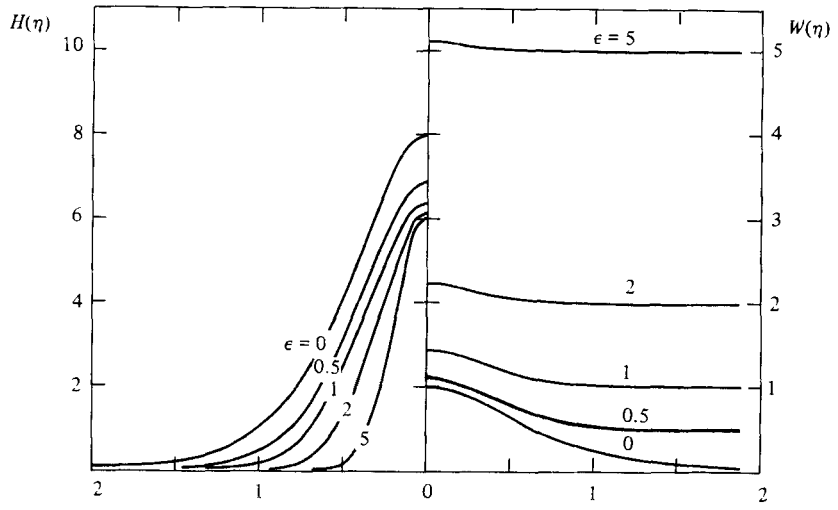

FIGURE 1. The dimensionless velocity W and temperature H for different ϵ-values.

ϵ	0	0.1	0.25	0.5	1.0	2.0	5.0
$H(0)$	8.000	7.708	7.313	6.848	6.390	6.128	6.023

TABLE 1. The dimensionless centreline temperature for different ϵ-values

giving
$$W = (1+\eta^2)^{-2}. \tag{2.13}$$

Here and in the rest of the paper, W denotes the dimensionless vertical velocity component, and we note that it has the same form as that for the momentum jet (see Batchelor & Gill, equation (1.5)).

For $\epsilon \neq 0$ we solved (2.9) and (2.10) numerically using the procedure outlined in Riley & Drake. In this paper we have restricted attention to the case of $\sigma = 1$ only. Figure 1 displays the graphs of H and W for $\epsilon = 0$, 0.5, 1, 2, and 5, whilst typical values of the dimensionless centerline temperature $H(0)$ are given in table 1. It is noteworthy that, for $\sigma = 1$ only,

$$\lim_{\eta \to 0} \frac{F'}{\eta} = (1+\epsilon^2)^{\frac{1}{2}}.$$

3. The stability equations

To investigate the stability of the basic flow, we follow the usual practice in linear stability theory of superimposing arbitrarily small perturbations to the base flow velocities, pressure and temperature, and invoking the parallel flow approximation. After using the scales (2.8) to non-dimensionalize the unsteady Boussinesq equations, the dimensionless perturbations are taken to have the form:

$$(\tilde{u}, \tilde{v}, \tilde{w}, \tilde{p}, \tilde{\theta}) = (\mathrm{i}\hat{u}, \hat{v}, \hat{w}, \hat{p}, \hat{\theta}) \exp\{\mathrm{i}(n\phi + \gamma(\tilde{z}) - \omega t)\}, \tag{3.1}$$

where $\hat{u}, \ldots, \hat{\theta}$ are functions of η, t is time, n is an integer and physical quantities correspond to the real part of complex functions. A temporal analysis is undertaken, so that the frequency ω is taken to be complex, whilst $\gamma(\tilde{z})$ is taken to be real. On introducing the base flow plus perturbations given by (3.1) into the full non-dimensional equations and letting $\tilde{z} \to \infty$ with η fixed, we obtain after linearization

$$\left(\frac{\mathrm{d}}{\mathrm{d}\eta}+\frac{1}{\eta}\right)\hat{u}+\frac{n}{\eta}\hat{v}+\alpha\hat{w}=0, \tag{3.2}$$

$$D\hat{u}=\mathrm{i}\frac{\mathrm{d}\hat{p}}{\mathrm{d}\eta}+\frac{1}{R}\left(\mathscr{T}\hat{u}-\frac{1}{\eta^2}\hat{u}-\frac{2n}{\eta^2}\hat{v}\right), \tag{3.3}$$

$$D\hat{v}=-\frac{\mathrm{i}n}{\eta}\hat{p}+\frac{1}{R}\left(\mathscr{T}\hat{v}-\frac{1}{\eta^2}\hat{v}-\frac{2n}{\eta^2}\hat{u}\right), \tag{3.4}$$

$$D\hat{w}+\mathrm{i}W'\hat{u}=-\mathrm{i}\alpha\hat{p}+\frac{1}{R}(\mathscr{T}\hat{w}+\hat{\theta}), \tag{3.5}$$

$$D\hat{\theta}+\mathrm{i}H'\hat{u}=\frac{1}{\sigma R}\mathscr{T}\hat{\theta}, \tag{3.6}$$

where

$$R=12\tilde{z}^{\frac{1}{2}}, \quad D=\mathrm{i}\alpha(W-c), \quad \mathscr{T}=\frac{\mathrm{d}^2}{\mathrm{d}\eta^2}+\frac{1}{\eta}\frac{\mathrm{d}}{\mathrm{d}\eta}-\frac{n^2}{\eta^2}-\alpha^2. \tag{3.7}$$

Here $\alpha=\tilde{z}^{\frac{1}{2}}\mathrm{d}\gamma/\mathrm{d}\tilde{z}$ denotes the dimensionless wavenumber and $c=\omega\tilde{z}^{\frac{1}{2}}L^*/\alpha U^*$ is a complex constant, whose real part represents dimensionless phase speed and whose imaginary part gives the growth rate. It should be stressed that (3.2)–(3.6) are obtained by invoking the parallel-flow approximation, which neglects all $\tilde{z}$-dependence via η in the base flow and the perturbations, relative to the exponential $\tilde{z}$-dependence $\mathrm{e}^{\mathrm{i}\gamma(\tilde{z})}$ in (3.1) – this follows from assuming that $\mathrm{d}\gamma/\mathrm{d}\tilde{z}=O(\tilde{z}^{-\frac{1}{2}})$ as $\tilde{z}\to\infty$. By neglecting the algebraic $\tilde{z}$-dependence in obtaining (3.2)–(3.6) some terms of order R^{-1} have been omitted from these equations. These terms, however, involve lower-order derivatives and so the retained viscous terms constitute the dominant terms in critical layer, whilst also allowing the full set of boundary conditions to be satisfied.

By eliminating the pressure and introducing new dependent variables, we obtain from (3.2)–(3.6)

$$\mathscr{D}^2\Phi=\mathrm{i}\alpha R\{(W-c)\mathscr{D}-\mathscr{D}_1 W\}\Phi+2\alpha n\mathscr{D}\Omega+\alpha\left\{\eta\frac{\mathrm{d}}{\mathrm{d}\eta}+\frac{2n^2}{\tilde{\eta}}\right\}\Theta, \tag{3.8}$$

$$\mathscr{L}\Omega=\mathrm{i}\alpha R(W-c)\Omega-\frac{n}{\tilde{\eta}}\left\{\frac{\mathrm{i}R}{\eta}W'+\frac{2\alpha}{\tilde{\eta}}\mathscr{D}\right\}\Phi+\frac{n}{\tilde{\eta}}\Theta, \tag{3.9}$$

$$\mathscr{T}\Theta=\mathrm{i}\alpha R\sigma(W-c)\Theta+\frac{\mathrm{i}\sigma}{\eta}RH'\Phi, \tag{3.10}$$

where

$$\left.\begin{aligned}\tilde{\eta}&=n^2+\alpha^2\eta^2, \quad \mathscr{D}_1=\frac{\mathrm{d}^2}{\mathrm{d}\eta^2}+\frac{n^2-\alpha^2\eta^2}{\tilde{\eta}}\frac{1}{\eta}\frac{\mathrm{d}}{\mathrm{d}\eta},\\ \mathscr{D}&=\mathscr{D}_1-\frac{\tilde{\eta}}{\eta^2}, \quad \mathscr{L}=\mathscr{D}+\frac{4\alpha^2\eta^2}{\tilde{\eta}}\frac{1}{\eta}\frac{\mathrm{d}}{\mathrm{d}\eta}.\end{aligned}\right\} \tag{3.11}$$

In the above,

$$\Omega(\eta)=\frac{\alpha\eta\hat{v}-n\hat{w}}{\tilde{\eta}}, \quad \Phi(\eta)=\eta\hat{u}, \quad \Theta(\eta)=\hat{\theta}. \tag{3.12}$$

When $n = 0$, Φ represents the amplitude of a Stokes stream function and $\Omega \equiv 0$. In the case of asymmetric disturbances Ω is related to the radial component of vorticity.

The conditions to be applied on (3.8)–(3.10) at $\eta = 0$ depend on n. If $n = 0$ the perturbation motion is toroid-like with

$$u = \frac{\partial w}{\partial \eta} = \frac{\partial p}{\partial \eta} = \frac{\partial \theta}{\partial \eta} = 0,$$

whilst $$w = p = \theta = 0 \quad \text{for} \quad n \geqslant 1$$

and $$u = v = 0 \quad \text{for} \quad n \geqslant 2,$$

because the velocity, pressure and temperature are single-valued. Thus the conditions satisfied by Ω, Φ and Θ are

$$\left.\begin{aligned} &\lim_{\eta\to 0} \frac{\Phi}{\eta} = \lim_{\eta\to 0} \left(\frac{\Phi'}{\eta}\right)' = \Theta'(0) = 0 \quad (n = 0), \\ &\lim_{\eta\to 0} \left(\Phi' - \frac{n\Phi}{\eta}\right) = \lim_{\eta\to 0} \mathscr{T}(\eta\Phi' - 2\Phi) = \Omega(0) = \Theta(0) = 0 \quad (n \geqslant 1). \end{aligned}\right\} \tag{3.13}$$

Furthermore, the perturbations must decay to zero as $\eta \to \infty$, giving

$$\left.\begin{aligned} &\frac{\Phi}{\eta} \to 0, \quad \frac{\Phi'}{\eta} \to 0, \quad \Theta \to 0 \quad \text{as} \quad \eta \to \infty \quad \text{for} \quad n \geqslant 0, \\ &\eta\Omega \to 0 \quad \text{as} \quad \eta \to \infty \quad \text{for} \quad n \geqslant 1. \end{aligned}\right\} \tag{3.14}$$

4. The eigenvalue problem

When solving the differential equations (3.8)–(3.10), the domain $[0, \infty)$ is divided into four:

$$\text{(i)}\ [0, \eta_s], \quad \text{(ii)}\ [\eta_s, \eta_m], \quad \text{(iii)}\ [\eta_m, \eta_a], \quad \text{(iv)}\ [\eta_a, \infty), \tag{4.1}$$

where $\eta_s < \eta_m < \eta_a$. In (i) the solution is determined as a power series satisfying (3.13), and in (iv) asymptotic solutions satisfying (3.14) are found in terms of modified Bessel functions. In (ii) and (iii) a Runge–Kutta Merson procedure is used to integrate numerically the equations from η_s to η_m and from η_a to η_m respectively. The initial conditions at η_s and η_a are given by evaluating the analytical solutions from regions (i) and (iv) respectively. At η_m continuity in Φ, $\mathrm{d}\Phi/\mathrm{d}\eta$, $\Psi = \mathscr{D}\Phi$, $\mathrm{d}\Psi/\mathrm{d}\eta$, Ω, $\mathrm{d}\Omega/\mathrm{d}\eta$, Θ and $\mathrm{d}\Theta/\mathrm{d}\eta$ is used and the two numerical solutions matched. The condition for solvability of the resulting equations then generates an eigenvalue relation of the form $G(\epsilon, \sigma, R, \alpha, c) = 0$. To satisfy this relation either α or c must be complex. We have taken c to be complex, i.e. $c = c_r + \mathrm{i}c_i$, where c_r is the phase speed and αc_i the growth rate of the disturbance. Further details concerning the methods of solution are given in the Appendix. In this section we now focus attention on aspects of the numerical results.

We first verified the numerical scheme by recalculating the stability characteristics of a round momentum jet, with neither temperature nor imposed flow involved. Batchelor & Gill showed that the velocity distribution may be approximated by the form given in (2.13). Our results confirmed those of Batchelor & Gill and of Burridge; our results may be more accurate than those of Burridge. The results for the

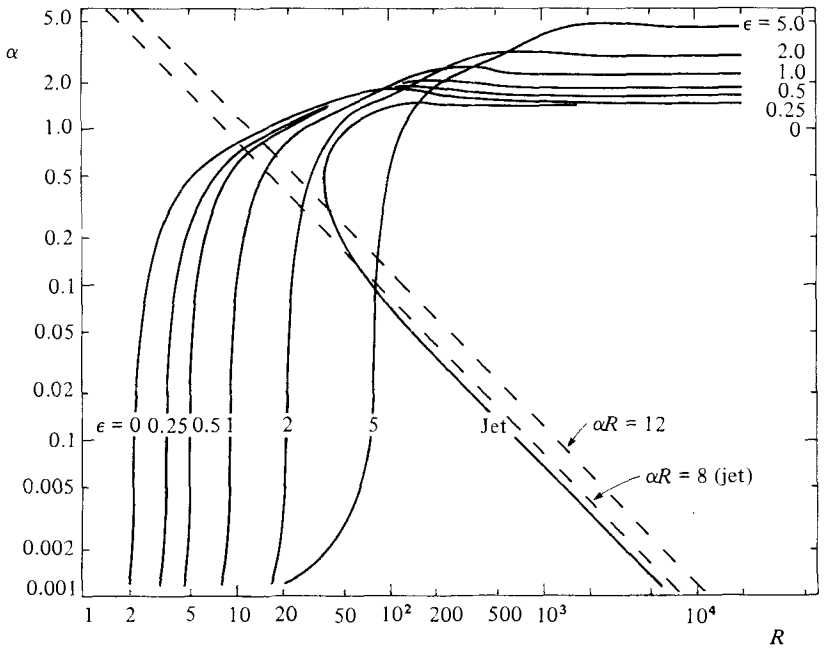

FIGURE 2. The neutral curves in the (α, R)-plane for a momentum jet and for plumes with different ϵ-values.

asymmetric mode $n = 1$ are presented in figure 2 (the curve labelled 'jet') and figure 3. Figure 2 shows the neutral stability curve ($c_i = 0$) in the (α, R)-plane for R up to 20000 and $\alpha > 0.001$. On the upper inviscid branch

$$\alpha \to 1.457, \quad c_r \to 0.621 \quad \text{as} \quad R \to \infty,$$

on the lower viscous branch

$$\alpha R \to 6.78 \quad c_r \to 0.063 \quad \text{as} \quad R \to \infty,$$

whilst the critical values were determined as

$$\alpha_c = 0.451, \quad R_c = 37.79, \quad (c_r)_c = 0.231.$$

The form of the lower branch means that solutions do not tend to those of the Rayleigh equation, but to a boundary-layer type of approximation to the stability equations, obtained by taking $\alpha R \to 6.78$ as $\alpha \to 0$ (see Gill & Davey 1969). Moreover the type of lower-branch analysis of Smith (1979) is not really a tractable proposition as there would be a difficult numerical problem involved.

Figure 3 presents the curves of constant c_r and c_i in the (α, R)-plane. For large R, the respective curves behave in much the same way, except for a small core with closed curves of constant c_i. The maximum values of c_i lie inside this core, which means that the disturbances with the corresponding wavenumbers have their largest growth rate at a finite Reynolds number. Our results are essentially the same as those of Burridge and our numerical procedure is therefore confirmed.

The mixed convection stability results for $n = 1$ are given in figures 2, 4, 5 and 6. Figure 2 shows the neutral curve for no forced flow ($\epsilon = 0$) and for five different

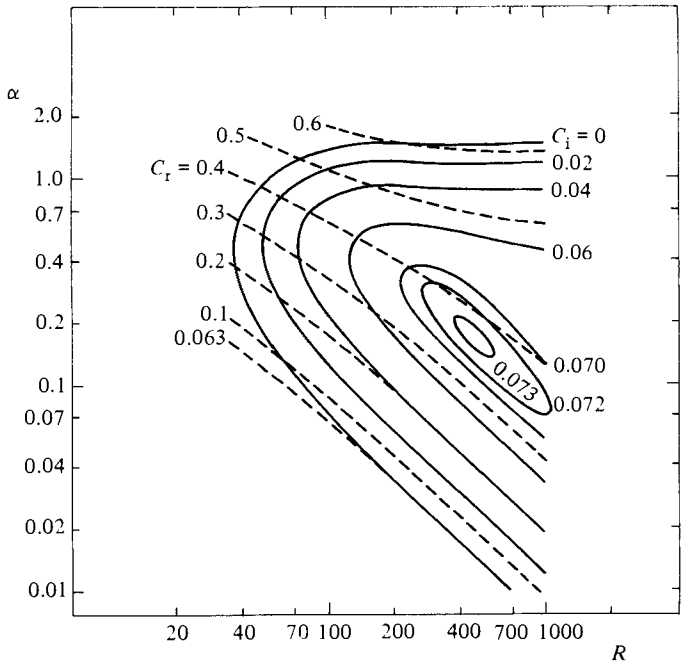

FIGURE 3. Curves of constant c_r and c_i in the (α, R)-plane for the momentum jet.

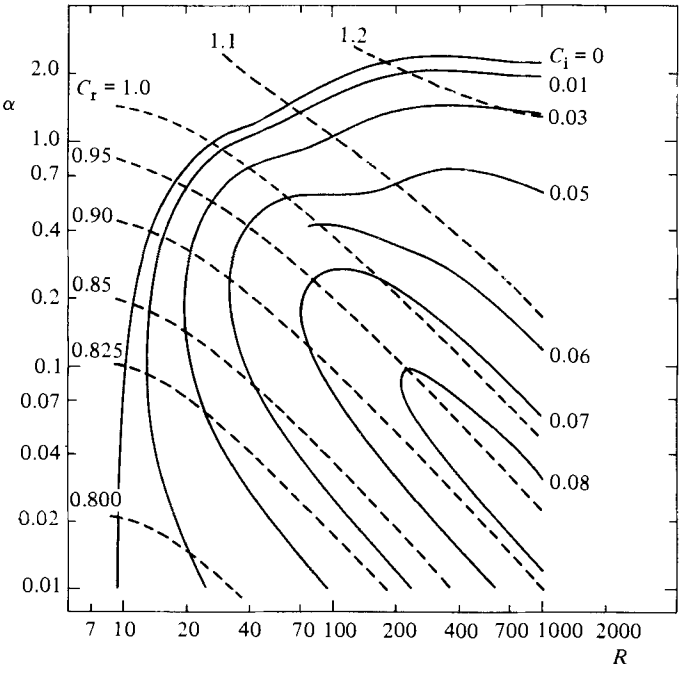

FIGURE 4. Curves of constant c_r and c_i in the (α, R)-plane for the plume with $\epsilon = 1.0$.

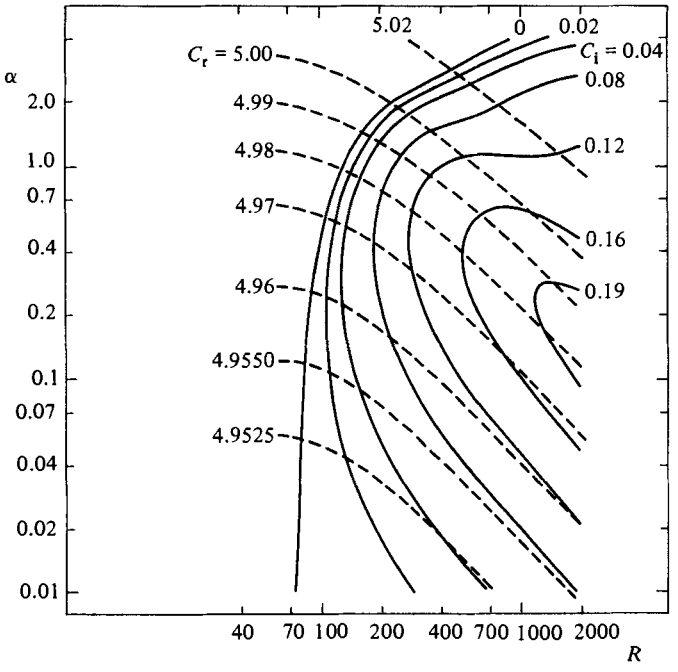

FIGURE 5. Curves of constant c_r and c_i in the (α, R)-plane for the plume with $\epsilon = 5.0$.

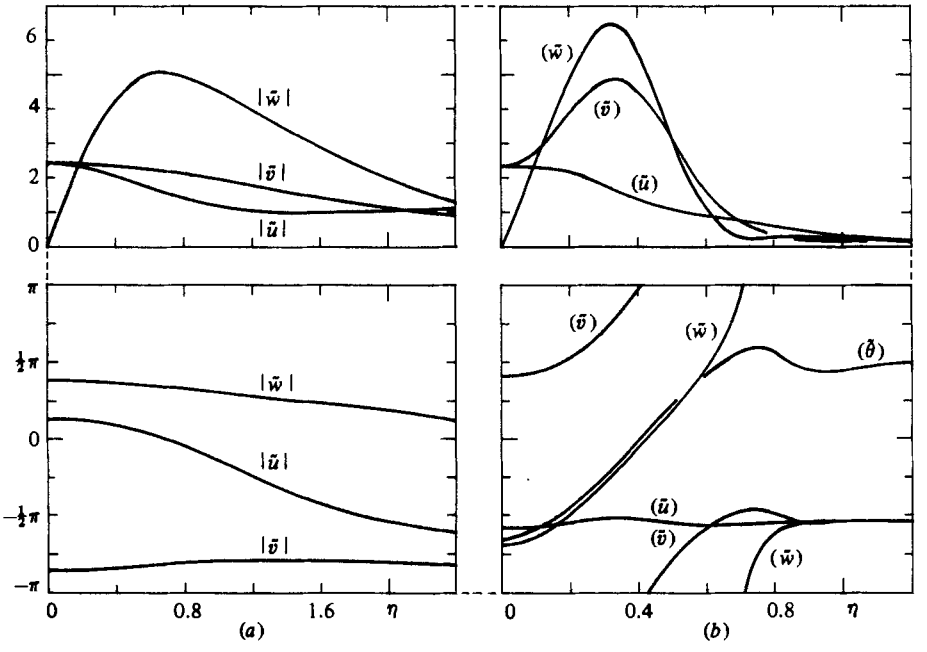

FIGURE 6. Neutrally stable eigenfunctions for $\epsilon = 1.0$. | | and ( ) denote amplitude and phase respectively. (*a*) $R = 20.298$, $\alpha = 0.80$; (*b*) $R = 1000$, $\alpha = 2.2524$.

ϵ	α_Q	$(c_r)_Q$	η_Q
0.0	1.457	0.621	0.519
0.25	1.621	0.715	0.489
0.50	1.830	0.862	0.451
1.0	2.270	1.240	0.380
2.0	2.994	2.135	0.294
5.0	4.627	5.056	0.192

TABLE 2. The limits, for different ϵ-values, of wavenumber α_Q and phase speed $(c_r)_Q$, as $R \to \infty$ along the upper neutral branch. The values of η_Q, the point where $W = c_r$, are also displayed.

strengths of forced flow. The main features are the same for all the curves. There is an upper inviscid branch with the same characteristics as for the jet, that is α and c_r tend to constants, α_Q and $(c_r)_Q$ say, as $R \to \infty$. We also find that $(c_r)_Q = W(\eta_Q)$, where η_Q is the point in the fluid at which

$$Q(\eta) = \frac{\eta W'}{n^2 + \alpha^2 \eta^2}$$

has a maximum (see table 2). This result is not surprising since the thermal coupling vanishes as $R \to \infty$, and we should expect to recover the result of Batchelor & Gill for inviscid jets.

Away from the upper branch, however, the neutral curves have little in common with the neutral curve for the jet. We find no critical point: R is strictly decreasing as α decreases down to $\alpha = 0.001$ (the lower limit of α in our computations). Now in our analysis we have employed the parallel-flow approximation, which is not a good approximation at small Reynolds numbers.† Thus our results cannot be regarded as valid quantitatively at the lower Reynolds numbers. Pera & Gebhart (1971) also found this in their study of the stability of two-dimensional thermal plumes. For that problem, however, Hieber & Nash (1975) were apparently able to find a critical Reynolds number by accounting for non-parallel effects in an asymptotic ($R \gg 1$) analysis.

We have limited the presentation of the constant c_r and c_i curves to the cases of $\epsilon = 1.0$ and $\epsilon = 5.0$ (figures 4 and 5 respectively). The curves for amplified disturbances are quite different from the neutral curve as $\alpha \to 0$. The behaviour is much the same as for the jet problem: for c_i not too small

$$\alpha R^{1+\delta} \to \text{constant} \quad \text{as} \quad R \to \infty,$$

where $\delta \ll 1$.

Figure 6 displays the amplitude and phase of the velocity components for neutral disturbances with $\epsilon = 1.0$ and at Reynolds numbers of (*a*) 20.3 and (*b*) 1000. (The temperature is not shown because $\tilde{\theta}$ has a similar behaviour to $\tilde{w}$.) At the smaller Reynolds number the velocities decay slowly from their maximum values. This is in sharp contrast with the large-Reynolds-number behaviour, where the changes with η are much more rapid. In this latter case, $\tilde{v}$ and $\tilde{w}$ have maxima at a distance from the centreline close to the point where $W = c$. Furthermore, changes in the phases of $\tilde{v}$ and $\tilde{w}$ (and $\tilde{\theta}$) are localized near this point. The tendency towards phase jumps in $\tilde{v}$, $\tilde{w}$ and $\tilde{\theta}$, but not in $\tilde{u}$, for increasing values of R may be seen from (3.8)–(3.10).

† In the mixed-convection case, Grashof number would perhaps be a more accurate description of R.

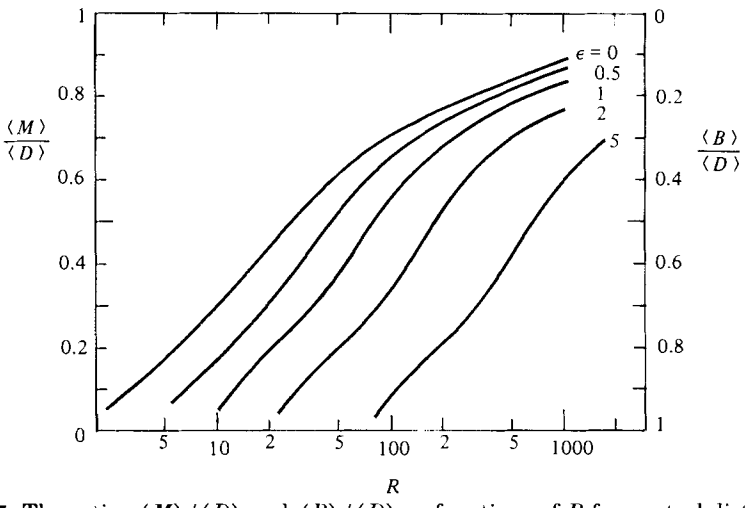

FIGURE 7. The ratios $\langle M\rangle/\langle D\rangle$ and $\langle B\rangle/\langle D\rangle$ as functions of R for neutral disturbances.

On letting $R\to\infty$, (3.8) yields a regular solution for Φ, but Ω and Θ become singular at η_Q. The eigenfunctions for other ϵ-values have a very similar behaviour.

For the symmetric case ($n = 0$) we found that all disturbances are damped, at least in the range of wavenumber considered. It is plausible that buoyancy-induced instability exists for very small α, but this is of little physical interest since the amplification rates are probably much larger for the asymmetric disturbances of moderate wavenumber. This remark regarding the $n = 0$ modes being stable also applies for modes with $n > 1$.

5. The perturbation energy

In order to gain some insight into the relative importance of mechanically driven and buoyancy-driven instabilities, the energy balance within a sinuous disturbance is now examined.

The derivation of the equation governing the disturbance energy is straightforward (see e.g. Nachtsheim 1963, p. 10). On omitting the details, it takes the form

$$2\alpha c_i\langle E\rangle = \langle M\rangle + \langle B\rangle - \langle D\rangle, \tag{5.1}$$

where

$$E = \tfrac{1}{2}|\hat{\boldsymbol{v}}|^2, \quad M = \frac{W'(\hat{u}\bar{\hat{w}} - \bar{\hat{u}}\hat{w})}{2\mathrm{i}}, \quad B = \frac{\bar{\hat{\theta}}\hat{w} - \hat{\theta}\bar{\hat{w}}}{2R},$$

$$D = \frac{1}{R}\left\{\left|\frac{\mathrm{d}\hat{\boldsymbol{v}}}{\mathrm{d}\eta}\right|^2 + 2\alpha^2 E + \frac{1}{\eta^2}(|\hat{w}|^2 + 2|\hat{u} + \hat{v}|^2)\right\},$$

$$\langle(\ )\rangle = \int_0^\infty \eta(\ )\,\mathrm{d}\eta, \quad \hat{\boldsymbol{v}} = (\hat{u}, \hat{v}, \hat{w}),$$

and the overbars denote complex conjugation.

$2\alpha c_i\langle E\rangle$ represents the rate of change of the kinetic energy of the disturbance, $\langle M\rangle$ the rate of transfer of kinetic energy from the mean flow to the disturbance, $\langle B\rangle$ the rate of gain of disturbance energy from potential energy (via the work done by

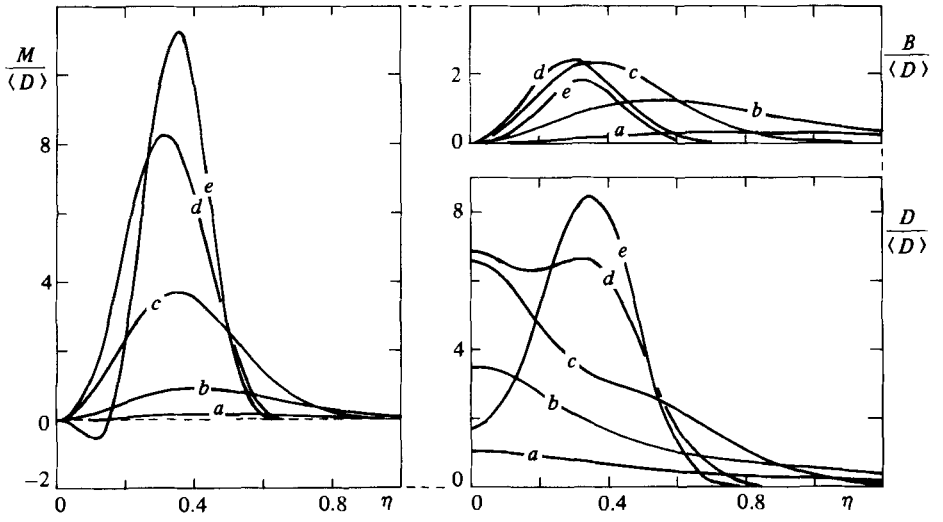

FIGURE 8. M, B and D as functions of η for $\epsilon = 1.0$, and for five different neutrally stable (α, R)-values: (*a*) (0.1, 10.137); (*b*) (1.0, 26.303); (*c*) (1.8982, 100); (*d*) (2.4431, 400); (*e*) (2.2524, 1000).

buoyancy forces), and $\langle D \rangle$ the rate of viscous dissipation. The dissipation term is always negative, so, if the sum of $\langle M \rangle$ and $\langle B \rangle$ is greater than $\langle D \rangle$, the right-hand side of (5.1) is positive, leading to instability. The left-hand side is zero for neutral disturbances, which is the case we now consider.

Figure 7 displays $\langle M \rangle / \langle D \rangle$ and $\langle B \rangle / \langle D \rangle$ as functions of the Reynolds number for various ϵ-values. When $\langle M \rangle$ is greater than $\langle B \rangle$, the transfer of kinetic energy from the basic flow dominates the process of conversion of potential energy, and vice versa. At small and moderate Reynolds numbers the instability is mainly of thermal origin, whereas for larger values it is mechanical. We note that $\langle B \rangle / \langle D \rangle \to 0$ as $R \to \infty$.

Furthermore, in order to study where the instability occurs, M, B and D are plotted as functions of η for different Reynolds numbers in figure 8. In this figure $\epsilon = 1.0$, but again the behaviour is similar for other ϵ-values. The maximum values of M and B are always at some distance from the centreline $\eta = 0$, whilst the dissipation D is largest at $\eta = 0$ for small and moderate Reynolds numbers, and away from $\eta = 0$ for large R. Moreover in this latter case, the maximum values of M, B and D coincide with those of the disturbance velocities, i.e. at the point where $W = c$.

6. Discussion

The original purpose of this investigation was to explain the stabilization of a plume by the introduction of a coflowing external stream. From a physical point of view the reasons for the stabilization may be found in figure 1. Two features are evident as the strength of the external flow increases: (i) the basic velocity profile flattens and (ii) the basic temperature difference across the plume decreases. Thus the local vorticity and the local potential energy in the plume are reduced by the introduction of the external stream. However, because of non-parallel-flow effects, the theoretical description is not complete. Figure 2 shows the difficulty clearly: we have superposed the curves $\alpha R = 8$ (jet) and $\alpha R = 12$ (plume with or without external stream), which

are curves representing the locus of points in the (α, R)-plane where the wavelength of the disturbance and the height above the source are of the same order. For our analysis to be valid, we should consider only disturbances of much shorter wavelengths than the height. This then shows the limitations of the approximation of parallel flow. It may be possible to extend the range of validity of our results by the type of analysis engaged in by Hieber & Nash or the more complete analyses of Smith and, more recently, Goldstein (1983). An encouraging aspect of our results (see e.g. figures 4 and 5) is that there does not appear to be any critical layer in the region of non-validity. However, also the Reynolds number is quite low, and so the use of asymptotic analysis for large values of the Reynolds number seems inappropriate. To mitigate this, note that the evidence concerning non-parallel effects is that they tend to stabilize, leading to some increase in the critical Reynolds number. As an example of a stabilizing non-parallel effect, we may cite the assumed temperature profile. In the parallel flow analysis it is taken to be independent of z, but, according to the similarity solution, it actually decreases like z^{-1}.

Finally, it is interesting to note that the Reynolds number is proportional to $z^{\frac{1}{2}}$. Thus, for fixed wavenumber, the 'stable length' of the plume is *quadrupled*, if the corresponding critical Reynolds number is *doubled* by the stabilizing forced flow.

The experimental work on this problem is not available on the open literature and so comparison with experiment is not possible here.

The authors wish to express their gratitude to Professor Philip Drazin for many stimulating discussions on this problem and for comments on the draft of this paper. M.T. also wishes to express his gratitude for the hospitality of the University of Bristol and to acknowledge support from the University of Oslo and NATO (through NTNF, Norway).

Appendix. The numerical solution of the stability problem

In this section results needed for and details of the numerical solution of (3.8)–(3.10) with the boundary conditions (3.13) and (3.14) are presented. It is convenient to transform (3.8) into two second-order equations by introducing $\Psi = \mathscr{D}\Phi$, giving

$$\mathscr{D}\Phi = \Psi, \tag{3.8a}$$

$$\mathscr{D}\Psi = \mathrm{i}\alpha R(W-c)\,\Psi - \mathrm{i}\alpha R(\mathscr{D}_1 W)\,\Phi + 2\alpha n\mathscr{D}\Omega + \alpha\left\{\eta\frac{\mathrm{d}}{\mathrm{d}\eta} + \frac{2n^2}{\tilde{\eta}}\right\}\Theta. \tag{3.8b}$$

A.1. *Asymptotic solutions for* $\eta \in [\eta_a, \infty)$, $\eta_a \gg 1$

From figure 1 we see that $W \to \epsilon$, $W' \to 0$ and $H' \to 0$ as $\eta \to \infty$. When $W = \epsilon$ and the terms involving $\mathscr{D}_1 W$, W' and H' are dropped from (3.8*b*), (3.9) and (3.10), four independent solutions satisfying the conditions at ∞ are

$$\Phi_1 = \alpha\eta K_n'(\alpha\eta), \quad \Psi_1 = \Omega_1 = \Theta_1 = 0, \tag{A 1}$$

$$\left.\begin{aligned} \Phi_2 &= \beta K_n'(\beta\eta), \quad \Omega_2 = \frac{n(\beta^2-\alpha^2)\,K_n(\beta\eta)}{\alpha\tilde{\eta}}, \\ \Psi_2 &= \mathscr{D}\Phi_2 = (\beta^2-\alpha^2)\,\Phi_2 + 2n\alpha\Omega_2, \quad \Theta_2 = 0. \end{aligned}\right\} \tag{A 2}$$

$$\left.\begin{aligned} \Phi_3 &= nK_n(\beta\eta), \quad \Omega_3 = -\frac{\alpha}{\tilde{\eta}}\beta\eta K_n'(\beta\eta). \\ \Psi_3 &= \mathscr{D}\Phi_3 = (\beta^2-\alpha^2)\,\Phi_3 + 2n\alpha\Omega_2, \quad \Theta_3 = 0. \end{aligned}\right\} \tag{A 3}$$

$$\left.\begin{aligned} \Phi_4 &= \frac{\tilde{\eta}}{2\alpha} K_n(\beta\eta) - \frac{\alpha}{\beta^2-\alpha^2}\beta\eta K_n'(\beta\eta), \quad \Omega_4 = 0, \\ \Psi_4 &= \mathscr{D}\Phi_4 = \frac{\tilde{\eta}}{2\alpha}\Theta_4, \quad \Theta_4 = (\beta^2-\alpha^2) K_n(\beta\eta). \end{aligned}\right\} \tag{A 4}$$

Here β is the root of $\alpha^2 + i\alpha R(\epsilon - c)$ with positive real part, and K_n is the modified Bessel function of order n. The general solution for $\eta \geqslant \eta_a$ is of the form

$$(\Phi, \Psi, \Omega, \Theta) = \sum_{j=1}^{4} A_j(\Phi_j, \Psi_j, \Omega_j, \Theta_j), \tag{A 5}$$

where $A_1, \ldots, A_4$ are constants to be determined.

A.2. *Series solutions for* $\eta \in [0, \eta_s]$, $\eta_s \ll 1$

Power-series solutions to (3.8*a*,*b*)–(3.10) satisfying the conditions at $\eta = 0$ exist in terms of η^2. Though these may be found for all values of n, we shall restrict the presentation to $n = 1$.

The base flow velocity and temperature W and H have series convergent for $|\eta| < 1$:

$$(W, H) = \sum_{j=0}^{\infty} (W_j, H_j)\, \eta^{2j},$$

where, for $\epsilon = 0$,

$$W_j = (-1)^j (j+1), \quad H_j = (-1)^j 3(j+1)(j+2).$$

When $\epsilon \neq 0$ the coefficients W_j and H_j are determined numerically. On taking into account the conditions (3.13), the series for Φ, Ψ, Ω and Θ may be written

$$(\Phi, \Psi, \Omega, \Theta) = \sum_{j=1}^{\infty} (a_j, b_j, d_j, h_j)\, \eta^{2j-1},$$

where the differential equations yield recurrence relations for the coefficients in terms of $a_1, \ldots, h_1$.

Four independent solutions $(\hat{\Phi}_j, \hat{\Psi}_j, \hat{\Omega}_j, \hat{\Theta}_j)$, $j = 1, \ldots, 4$, are generated by taking $a_1 = \delta_{1j}$, $b_1 = \delta_{2j}$, $d_1 = \delta_{3j}$ and $h_1 = \delta_{4j}$, where δ is the Kronecker delta. The general solution for $\eta \leqslant \eta_s$ may then be written

$$(\Phi, \Psi, \Omega, \Theta) = \sum_{j=1}^{4} B_j(\hat{\Phi}_j, \hat{\Psi}_j, \hat{\Omega}_j, \hat{\Theta}_j), \tag{A 6}$$

where $B_1, \ldots, B_4$ are constants to be determined.

A.3. *Numerical integration from* η_s *to* η_m *and from* η_a *to* η_m

Equations (3.8*a*,*b*)–(3.10) may be written in the equivalent form

$$\boldsymbol{Y}' = \boldsymbol{A}\boldsymbol{Y}, \tag{A 7}$$

where $\boldsymbol{A}$ is a square matrix of order 8 and

$$\boldsymbol{Y} = (\Phi, \Phi', \Psi, \Psi', \Omega, \Omega', \Theta, \Theta'),$$

with the prime denoting differentiation with respect to η.

Using the series solutions from §A.2, (A 7) may be integrated from η_s to η_m to give

$$\boldsymbol{Y} = \sum_{j=1}^{4} B_j \hat{\boldsymbol{Y}}_j,$$

ϵ	η_s	η_m	η_a	N_{sm}	N_{am}
0	0.1	1.0	10.0	3	19
0.25	0.1	1.0	5.0	3	9
0.50	0.1	1.0	3.50	5	11
1.0	0.1	1.0	3.00	5	9
2.0	0.01	0.50	1.75	3	6
5.0	0.01	0.25	1.25	5	17

TABLE 3. The values of η_s, η_m and η_a for different ϵ-values. N_{sm} and N_{am} give the maximum number of orthonormalizations in the intervals $[\eta_s, \eta_m]$ and $[\eta_m, \eta_a]$ respectively.

and similarly, using the asymptotic solutions from §A.1 and integrating from η_a to η_m gives

$$\boldsymbol{Y} = \sum_{j=1}^{4} A_j \boldsymbol{Y}_j.$$

Here the constants A_j and B_j are as in (A 5) and (A 6). Assuming continuity in $\boldsymbol{Y}$ at η_m yields the relation $G(\epsilon, \sigma, R, \alpha, c) = 0$ for solvability. The secant method is then used to determine the eigenvalue c for given values of ϵ, α and R.

A.4. *Orthonormalization*

The local solutions for $\eta \in [\eta_s, \eta_a]$ are composed of terms of the form $\exp(\pm\alpha_1\eta)$ and $\exp(\pm\beta_1\eta)$, where, in general, $|\beta_1| \gg |\alpha_1|$. Therefore when integrating from η_s to η_m the $\exp(\beta\eta)$-terms very soon dominate the other terms, giving dependent solutions. To avoid this, the four solutions $\boldsymbol{Y}_j$ are orthonormalized at equally spaced points η_s, $\eta_{s1}, \eta_{s2}, \ldots, \eta_m$. Similar considerations apply for the integration from η_a to η_m. In table 3 the maximum number of orthonormalization points in the calculations are displayed; the number depends on ϵ, R and α.

REFERENCES

BATCHELOR, G. K. & GILL, A. E. 1962 Analysis of the stability of axisymmetric jets. *J. Fluid Mech.* **14**, 529.

BURRIDGE, D. 1969 The instability of round jets. Ph.D. thesis, Bristol University.

BURRIDGE, D. 1970 The instability of round jets. *Florida State University Tech. Rep.* 29.

FUJII, T., MORIOKA, I. & SUZAKI, K. 1972 *Trans JSME* **38**, 2119.

GILL, A. E. & DAVEY, A. 1969 Instabilities of a buoyancy-driven system. *J. Fluid Mech.* **35**, 775.

GOLDSTEIN, M. E. 1983 The evolution of Tollmien–Schlichting waves near a leading edge. *J. Fluid Mech.* **127**, 59.

HIEBER, C. A. & NASH, E. J. 1975 Natural convection above a line heat source: higher-order effects and stability. *Intl J. Heat Mass Transfer* **18**, 1473.

MOLLENDORF, J. C. & GEBHART, B. 1973 An experimental and numerical study of the viscous stability of a round laminar vertical jet with and without buoyancy for symmetric and asymmetric disturbances. *J. Fluid Mech.* **61**, 367.

NACHTSHEIM, P. R. 1963 Stability of free-convection boundary layer flows. *NACA TN* D-2089.

PERA, L. & GEBHART, B. 1971 On the stability of laminar plumes: some numerical solutions and experiments. *Intl J. Heat Mass Transfer* **14**, 975.

RILEY, D. S. & DRAKE, D. G. 1983 Mixed convection in an axisymmetric buoyant plume. *Q. J. Mech. Appl. Maths* **36**, 43.

SHLIEN, D. J. & BOXMAN, R. L. 1979 Temperature field measurement of an axisymmetric laminar plume. *Phys. Fluids* **22**, 631.

SMITH, F. T. 1979 On the non-parallel flow stability of the Blasius boundary layer. *Proc. R. Soc. Lond.* A **366**, 91.

WAKITANI, S. 1980 The stability of a natural convection flow above a point heat source. *J. Phys. Soc. Japan* **49**, 2392.

YIH, C-S. 1977 *Fluid Mechanics*. West River.